Near-Field Source Localization: Sparse Recovery Techniques and Grid Matching

Keke Hu, Sundeep Prabhakar Chepuri, and Geert Leus
Faculty of Electrical Engineering, Mathematics and Computer Science,
Delft University of Technology, The Netherlands.
Email: {s.p.chepuri;g.j.t.leus}@tudelft.nl.

***Abstract*—Near-field source localization is a joint direction-of-arrival (DOA) and range estimation problem. Leveraging the sparsity of the spatial spectrum, and gridding along the DOA and range domain, the near-field source localization problem can be casted as a linear sparse regression problem. However, this would result in a very large dictionary. Using the Fresnel-approximation, the DOA and range naturally decouple in the correlation domain. This allows us to solve two inverse problems of a smaller dimension instead of one higher dimensional problem. Furthermore, the sources need not be exactly on the predefined sampling grid. We use a mismatch model to cope with such off-grid sources and present estimators for grid matching.**

***Index Terms*—Near-field, sparse recovery, direction-of-arrival, ranging, Fresnel approximation, grid matching.**

I. Introduction

Source localization is important for location-aware services, and has many applications in the field of seismology, acoustics, radar, sonar, and oceanography. Source localization can be categorized into two types, based on the distance between the source and the antenna array: (a) far-field (when $r \geq 2D^2/\lambda$), and (b) near-field source localization, where r is the range between the source and the phase-reference of the array, D is the array aperture, and λ is the wavelength of the source signal. In far-field source localization, the wavefront of the signal impinging on the array is assumed to be planar [1]. However, the curvature of the wavefront is no longer planar when sources are located close to the array, i.e., in the near field ($r \leq 0.62\sqrt{D^3/\lambda}$) or Fresnel region ($0.62\sqrt{D^3/\lambda} < r < 2D^2/\lambda$). Therefore, the algorithms that depend on the planar-wave assumption for direction-of-arrival (DOA) estimation are no longer valid. In this work, we focus on near-field source localization, which is achieved by a joint DOA and range (distance between the source and the phase-reference of the array) estimation.

Traditional approaches to near-field localization involve extending techniques like multiple signal classification (MUSIC) to a two-dimensional field [2]. A quadratic approximation (the so-called Fresnel approximation) of the wavefront is suggested in [3]. Using the Fresnel approximation, the rotational invariance property can be exploited between the symmetric subarrays to estimate the DOA using ESPRIT [4], and based on the estimated DOA, the range is subsequently estimated using MUSIC. In [5], which is closely related to our work, using the second-order statistics, the DOA and range are jointly estimated by finding the roots of a polynomial related to the correlations. However, they do not solve two one-dimensional inverse problems as presented in this paper.

This work was supported in part by STW under the FASTCOM project (10551) and in part by NWO-STW under the VICI program (10382).

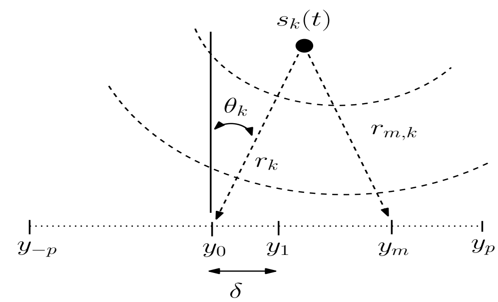

Fig. 1: A linear array receiving a signal from a near-field source.

We localize multiple narrowband near-field sources by estimating their DOA and range. Using the sparse representation framework, we form an overcomplete basis constructed using a sampling grid that is related to the possible source locations. By doing so, the original non-linear parameter estimation problem is transformed into a linear ill-posed problem. However, when the sources are not exactly on the predefined grid, the performance of the estimator is significantly affected. We account for such off-grid sources using a mismatch model, and provide estimators for grid matching. Using the Fresnel approximation and assuming that the sources are uncorrelated, we can decouple the DOA and range in the correlation domain. This allows us to significantly reduce the complexity, by solving two inverse problems of smaller dimensions one by one, instead of solving one inverse problem of a higher dimension. More specifically, we first estimate the DOA and then use the estimated DOA for range estimation. The error due to Fresnel approximation is significant when the sources are in near-field (i.e., $r \leq 0.62\sqrt{D^3/\lambda}$). We provide an algorithm based on non-linear least-squares (NLS) to minimize this approximation error.

II. Signal model

Consider K narrowband sources present in the near field impinging on an array of $M = 2p + 1$ sensors as illustrated in Fig. 1. Without loss of generality, it is assumed that the phase reference of the array is at the origin, and the sensors are placed at location indices in the range $[-p, p]$. Denoting the spacing between two adjacent sensors as δ, the position

978-1-4799-1481-4/14/$31.00

of the m-th sensor will be $m\delta$ where $m \in [-p, p]$. The signal received by the m-th sensor at time t can be expressed as

$$y_m(t) = \sum_{k=1}^{K} s_k(t) \exp(j\frac{2\pi}{\lambda}(r_{m,k} - r_k)) + w_m(t), \quad (1)$$

where

$$r_{m,k} = \sqrt{r_k + m^2\delta^2 - 2m\delta r_k \sin(\theta_k)} \quad (2)$$

represents the distance between the mth sensor and the kth source, r_k is the range from the kth source to the phase reference, $s_k(t)$ is the signal radiated by the kth source characterized by the DOA-range pair (θ_k, r_k), λ denotes the wavelength, and $w_m(t)$ denotes i.i.d. Gaussian noise. We model the signal power of the kth source as $\mathbb{E}_t\{s_k(t)s_k^*(t)\} = \sigma_{s,k}^2$, and the noise power as $\mathbb{E}_t\{w_m(t)w_m^*(t)\} = \sigma_w^2$. Stacking the measurements in $\mathbf{y}(t) = [y_{-p}(t), \ldots, y_p(t)]^T \in \mathbb{C}^{M\times 1}$, we get

$$\mathbf{y}(t) = \sum_{k=1}^{K} \mathbf{a}(\theta_k, r_k)s_k(t) + \mathbf{w}(t), \quad \text{for} \quad t = t_1, \ldots, t_T, \quad (3)$$

where T denotes the number of snapshots, $\mathbf{a}(\theta_k, r_k) \in \mathbb{C}^{M\times 1}$ is the *steering vector*, and $\mathbf{w}(t) = [w_{-p}(t), \ldots, w_p(t)]^T \in \mathbb{C}^{M\times 1}$ is the noise vector.

Assuming the source signals are mutually uncorrelated, we can stack all the available spatial correlations into a vector $\mathbf{z} = \mathrm{vec}(\mathbb{E}\{\mathbf{y}(t)\mathbf{y}(t)^H\})$ of length $M^2 \times 1$, i.e.,

$$\mathbf{z} = \mathbf{\Phi}(\boldsymbol{\theta}, \mathbf{r})\mathbf{r}_s + \sigma_w^2\mathbf{e}, \quad (4)$$

where $\mathbf{\Phi}(\boldsymbol{\theta}, \mathbf{r}) = [\mathbf{a}^*(\theta_1, r_1) \otimes \mathbf{a}(\theta_1, r_1), \ldots, \mathbf{a}^*(\theta_K, r_K) \otimes \mathbf{a}(\theta_K, r_K)] \in \mathbb{C}^{M^2\times K}$ (the notation $\otimes$ denotes the Kronecker product), $\mathbf{r}_s = [\sigma_{s,1}^2, \ldots, \sigma_{s,K}^2]^T \in \mathbb{C}^{K\times 1}$, and $\mathbf{e} = \mathrm{vec}(\mathbf{I}_M)$. In practice, the vector $\mathbf{z}$ containing the statistical correlations is approximated using the measurements from (3).

The matrix $\mathbf{\Phi}$ depends on the unknown variables $(\boldsymbol{\theta}, \mathbf{r})$. By discretizing the θ-interval and r-interval using a known sampling grid, we can cast the joint DOA-range estimation problem as a sparse reconstruction problem. However, such a two-dimensional gridding results in a very huge dictionary and increases the complexity. In this paper, we propose to reduce the involved computational complexity by solving two inverse problems of smaller dimension. We do this by exploiting the spatial cross-correlation between the symmetric sensors, and using the fact that the structure of the Fresnel approximated model naturally decouples the DOA and range in the correlation domain.

III. Fresnel approximation

Using the second order Taylor expansion of (2), we get the so-called *Fresnel* approximation, which is given by

$$r_{m,k} \approx r_k - m\delta \sin\theta_k + m^2\delta^2 \frac{\cos^2\theta_k}{2r_k}.$$

We can now approximate $\tau_{m,k} \approx \frac{2\pi}{\lambda}(r_{m,k} - r_k)$ as

$$\begin{aligned} \tau_{m,k} &= -m\frac{2\pi\delta}{\lambda}\sin(\theta_k) + m^2\frac{\pi\delta^2}{\lambda r_k}\cos^2(\theta_k) \\ &= m\omega_k + m^2\phi_k \end{aligned} \quad (5)$$

where we re-parameterize the DOA and range, respectively as $\omega_k = -\frac{2\pi\delta}{\lambda}\sin(\theta_k)$ and $\phi_k = \frac{\pi\delta^2}{\lambda r_k}\cos^2(\theta_k)$. Substituting $\tau_{m,k}$ in (1), we get

$$y_m(t) \approx \sum_{k=1}^{K} s_k(t)e^{j(m\omega_k + m^2\phi_k)} + w_m(t).$$

This approximation is reasonable when the sources are in the Fresnel region.

IV. Two-step estimator with grid matching

The spatial correlation between the mth and nth sensor based on the Fresnel approximation can be written as

$$\begin{aligned} r_y(m, n) &= \mathbb{E}_t\{y_m(t)y_n^*(t)\} \\ &= \sum_{k=1}^{K} \sigma_{s,k}^2 e^{j(m-n)\omega_k + j(m^2-n^2)\phi_k} + \sigma_w^2\delta(m - n) \end{aligned}$$

where $\delta(.)$ represents the Dirac function. Notice that when $n = -m$ the spatial correlation is independent of the parameter ϕ_k [5], and we arrive at

$$\begin{aligned} r_y(-m, m) &= \mathbb{E}_t\{y_{-m}(t)y_m^*(t)\} \\ &= \sum_{k=1}^{K} \sigma_{s,k}^2 e^{-2m\omega_k j} + \sigma_w^2\delta(-2m). \end{aligned} \quad (6)$$

This means that by exploiting the cross-correlation between the symmetric sensors, we can transform the original two-dimensional (DOA and range) estimation into a one-dimensional (DOA) estimation. Stacking (6) for all the symmetric sensors, we can build a *virtual far-field* model:

$$\mathbf{r}_y = \mathbf{A}_\omega(\boldsymbol{\theta})\mathbf{r}_s + \sigma_w^2\mathbf{e}_1, \quad (7)$$

where $\mathbf{r}_y = [r_y(-p, p), \ldots, r_y(0, 0), \ldots, r_y(p, -p)]^T \in \mathbb{C}^{M\times 1}$, and $\mathbf{e}_1 = [\mathbf{0}_p^T, 1, \mathbf{0}_p^T]^T \in \mathbb{C}^{M\times 1}$, and the corresponding virtual array gain pattern for the kth source denoted by $\mathbf{a}_\omega(\omega_k)$ can be expressed as $\mathbf{a}_\omega(\omega_k) = [e^{-j2p\omega_k}, \ldots, 1, \ldots, e^{j2p\omega_k}]^T \in \mathbb{C}^{M\times 1}$, with the array manifold $\mathbf{A}_\omega(\boldsymbol{\theta}) = [\mathbf{a}_\omega(\theta_1), \ldots, \mathbf{a}_\omega(\theta_K)] \in \mathbb{C}^{M\times K}$. In practice, the vector $\mathbf{r}_y$ containing the statistical correlations is approximated using the measurements from (3).

A. Step-1: DOA estimation

We can construct an overcomplete basis $\mathbf{A}_\omega$ with N_θ potential source directions-of-arrival (DOAs) using the sampling grid $\bar{\boldsymbol{\theta}} = [\bar{\theta}_1, \bar{\theta}_2, \ldots, \bar{\theta}_{N_\theta}]^T$ of resolution τ_θ, i.e.,

$$\mathbf{A}_\omega(\bar{\boldsymbol{\theta}}) = [\mathbf{a}_\omega(\bar{\theta}_1), \ldots, \mathbf{a}_\omega(\bar{\theta}_{N_\theta})] \in \mathbb{C}^{M\times N_\theta},$$

where $\bar{\omega}_n = -\frac{2\pi\delta}{\lambda}\sin(\bar{\theta}_n)$ for all $n \in \{1, \ldots, N_\theta\}$ as defined earlier. The signal is represented by an $N_\theta \times 1$ vector $\mathbf{u}$, where every source can be found as a non-zero weight $u_n = \sigma_{s,k}^2$ if source k comes from direction $\bar{\theta}_n$ for some k and is zero otherwise. The discrete grid-based model in the correlation domain is then given by

$$\mathbf{r}_y = \mathbf{A}_\omega(\bar{\boldsymbol{\theta}})\mathbf{u} + \sigma_w^2\mathbf{e}_1. \quad (8)$$

Note that the number of potential source DOAs N_θ will typically be much greater than the number of sensors M, and the model in (8) is ill-posed. However, assuming that the spatial spectrum is sparse, we can solve for the unknown vector $\mathbf{u}$ using an ℓ_1-regularized least-squares (LS) minimization problem which is given by

$$\hat{\mathbf{u}} = \arg\min_{\mathbf{u}} \|\mathbf{r}_y - \mathbf{A}_\omega(\bar{\boldsymbol{\theta}})\mathbf{u}\|_2^2 + \mu\|\mathbf{u}\|_1, \tag{9}$$

where μ is the sparsity regulating parameter. However, the model in (8) is exact, only when the targets are located exactly on the sampling grid, which otherwise significantly deteriorates the performance of the estimator.

The accurate model is expressed using an unknown perturbation $\boldsymbol{\alpha} = [\alpha_1, \ldots, \alpha_{N_\theta}]^T$ around the sampling grid as

$$\mathbf{r}_y = \mathbf{A}_\omega(\bar{\boldsymbol{\theta}} + \boldsymbol{\alpha})\mathbf{u} + \sigma_w^2\mathbf{e}_1, \tag{10}$$

with $-0.5\tau_\theta \leq \alpha_n \leq 0.5\tau_\theta$ for $n = 1, \ldots, N_\theta$. Using the first-order Taylor expansion around the sampling grid $\bar{\boldsymbol{\theta}}$, we arrive at

$$\mathbf{A}_\omega(\bar{\boldsymbol{\theta}} + \boldsymbol{\alpha}) = \mathbf{A}_\omega(\bar{\boldsymbol{\theta}}) + \mathbf{D}_\omega\boldsymbol{\Delta}_\alpha, \tag{11}$$

where $\mathbf{D}_\omega = [\frac{\partial \mathbf{a}_\omega(\bar{\theta}_1)}{\partial \bar{\theta}_1}, \ldots, \frac{\partial \mathbf{a}_\omega(\bar{\theta}_{N_\theta})}{\partial \bar{\theta}_{N_\theta}}]$, and $\boldsymbol{\Delta}_\alpha = \mathrm{diag}(\boldsymbol{\alpha})$. Using the approximation (11) in (10) we have

$$\mathbf{r}_y = (\mathbf{A}_\omega(\bar{\boldsymbol{\theta}}) + \mathbf{D}_\omega\boldsymbol{\Delta}_\alpha)\mathbf{u} + \sigma_w^2\mathbf{e}_1. \tag{12}$$

As earlier, assuming that the spatial spectrum is sparse, the unknown $\mathbf{u}$ and $\boldsymbol{\alpha}$ can be solved using

$$\begin{aligned} \arg\min_{\mathbf{u},\boldsymbol{\alpha}} \; & \|\mathbf{r}_y - (\mathbf{A}_\omega(\bar{\boldsymbol{\theta}}) + \mathbf{D}_\omega\boldsymbol{\Delta}_\alpha)\mathbf{u}\|_2^2 + \mu_2\|\mathbf{u}\|_1, \\ \text{s.t.} \quad & \boldsymbol{\Delta}_\alpha = \mathrm{diag}(\boldsymbol{\alpha}), \mathbf{u} \geq \mathbf{0}, \\ & -0.5\tau_\theta \leq \alpha_n \leq 0.5\tau_\theta, \quad n = 1, \ldots, N_\theta. \end{aligned} \tag{13}$$

The optimization problem in (13) is non-convex, however, can be solved using alternating minimization [6] using the following iterations

$$\begin{aligned} \mathbf{u}[i+1] = & \arg\min_{\mathbf{u}} \|\mathbf{r}_y - (\mathbf{A}_\omega(\bar{\boldsymbol{\theta}}) + \mathbf{D}_\omega\boldsymbol{\Delta}_\alpha[i])\mathbf{u}\|_2^2 + \mu_2\|\mathbf{u}\|_1, \\ & \text{s.t.} \quad \boldsymbol{\Delta}_\alpha[i] = \mathrm{diag}(\boldsymbol{\alpha}[i]), \mathbf{u} \geq \mathbf{0}, \end{aligned} \tag{14a}$$

$$\begin{aligned} \boldsymbol{\alpha}[i+1] = & \arg\min_{\boldsymbol{\alpha}} \|\mathbf{r}_y - (\mathbf{A}_\omega(\bar{\boldsymbol{\theta}}) + \mathbf{D}_\omega\boldsymbol{\Delta}_\alpha)\mathbf{u}[i+1]\|_2^2, \\ & \text{s.t.} \quad \boldsymbol{\Delta}_\alpha = \mathrm{diag}(\boldsymbol{\alpha}), \\ & \qquad -0.5\tau_\theta \leq \alpha_n \leq 0.5\tau_\theta, \, n = 1, \ldots, N_\theta, \end{aligned} \tag{14b}$$

where we initialize $\boldsymbol{\alpha}[0] = \mathbf{0}_{N_\theta}$.

Alternatively, by letting $\mathbf{u}_\theta = \mathbf{u} \odot \boldsymbol{\alpha}$ (the notation $\odot$ denotes the elementwise Hadamard product), we can formulate a joint sparse recovery problem [7], [8] to solve the inverse problem in (12), and the resulting convex optimization problem is given as

$$\begin{aligned} \arg\min_{\mathbf{x}} \; & \|\mathbf{r}_y - \mathbf{A}_\omega(\bar{\boldsymbol{\theta}})\mathbf{u} - \mathbf{D}_\omega\mathbf{u}_\theta\|_2^2 + \mu_3\|\mathbf{x}\|_{2,1}, \\ \text{s.t.} \quad & \mathbf{x} = [\mathbf{u}^T, \mathbf{u}_\theta^T]^T, \mathbf{u} \geq \mathbf{0}, \\ & -0.5\tau_\theta \leq \alpha_n \leq 0.5\tau_\theta, \quad n = 1, \ldots, N_\theta, \end{aligned} \tag{15}$$

where $\|\mathbf{x}\|_{2,1} = \sum_{n=1}^{N_\theta} \sqrt{u_n^2 + u_{n,\theta}^2}$ with $\mathbf{u} = [u_1, \ldots, u_{N_\theta}]^T$, and $\mathbf{u}_\theta = [u_{1,\theta}, \ldots, u_{N_\theta,\theta}]^T$.

B. DOA correction

Let $\hat{\boldsymbol{\theta}}$ collect the estimated DOAs from step-1, and $\hat{K}$ denote the number of detected DOAs. Every estimated DOA suffers from the Fresnel approximation error along with the estimation error. We next refine the estimated DOA from step-1 by solving an NLS problem to minimize the Fresnel approximation error.

Using the DOA estimates in the Fresnel approximated delay in (5), we have,

$$\tau_{m,k} = -m\frac{2\pi\delta}{\lambda}\sin(\hat{\theta}_k) + m^2\frac{\pi\delta^2}{\lambda r_k}\cos^2(\hat{\theta}_k), k \in \{1, \ldots, \hat{K}\}.$$

We eliminate the unknown r_k by considering the difference delay between the mth and $-m$th sensor, i.e.,

$$b_m(\hat{\theta}_k) = \tau_{-m,k} - \tau_{m,k} = 2m\frac{2\pi\delta}{\lambda}\sin(\hat{\theta}_k).$$

Let the corresponding true difference delay be $f_m(\theta_k, r_k) = \frac{2\pi}{\lambda}(r_{-m,k} - r_{m,k})$. Collecting $f_m(\theta_k, r_k)$ for all $m \in [-p, p]$ we get the following non-linear equations

$$\mathbf{f}(\theta_k, r_k) = \mathbf{b}(\hat{\theta}_k), \tag{16}$$

where $\mathbf{f}(\theta_k, r_k) = [f_{-p}(\theta_k, r_k), \ldots, f_p(\theta_k, r_k)]^T \in \mathbb{R}^M$, and $\mathbf{b}(\hat{\theta}_k) = [b_{-p}(\hat{\theta}_k), \ldots, b_p(\hat{\theta}_k)]^T \in \mathbb{R}^M$.

By discretizing the range into N_r bins of resolution τ_r we have a range grid $\bar{\mathbf{r}} = [\bar{r}_1, \ldots, \bar{r}_{N_r}]^T \in \mathbb{R}^{N_r}$. For a fixed point in the range grid and for every detected DOA from step-1, we can solve (16) using an NLS estimator, i.e.,

$$\check{\theta}_{k,n} = \arg\min_{\theta_k} \|\mathbf{f}(\theta_k, \bar{r}_n) - \mathbf{b}(\hat{\theta}_k)\|_2^2, \tag{17}$$

for $k \in \{1, \ldots, \hat{K}\}$, and $n \in \{1, \ldots, N_r\}$. The non-linear optimization problem in (17) can be solved using Gauss-Newton's method initialized with the estimate from step-1. For estimating the range, we use the sampling grid $(\check{\boldsymbol{\theta}}, \bar{\mathbf{r}}) = \{(\check{\theta}_{1,1}, \bar{r}_1), (\check{\theta}_{2,1}, \bar{r}_1), \ldots, (\check{\theta}_{\hat{K},1}, \bar{r}_1), \ldots, (\check{\theta}_{\hat{K},N_r}, \bar{r}_{N_r})\}$.

C. Step-2: range estimation

Using the sampling grid $(\check{\boldsymbol{\theta}}, \bar{\mathbf{r}})$ in (4), we form an overcomplete basis $\boldsymbol{\Phi}(\check{\boldsymbol{\theta}}, \bar{\mathbf{r}}) \in \mathbb{C}^{M^2 \times \hat{K}N_r}$ to arrive at

$$\mathbf{z} = \boldsymbol{\Phi}(\check{\boldsymbol{\theta}}, \bar{\mathbf{r}})\mathbf{p} + \sigma_w^2\mathbf{e}, \tag{18}$$

where the signal is represented by a $\hat{K}N_r \times 1$ vector $\mathbf{p}$. The source DOA-range pair can be found as a non-zero weight of $\mathbf{p}$, by solving the optimization problem

$$\hat{\mathbf{p}} = \arg\min_{\mathbf{p}} \|\mathbf{z} - \boldsymbol{\Phi}(\check{\boldsymbol{\theta}}, \bar{\mathbf{r}})\mathbf{p}\|_2^2 + \mu_4\|\mathbf{p}\|_1. \tag{19}$$

However, there is no reason to believe that the targets are located exactly on the assumed range grid $\bar{\mathbf{r}}$. The accurate model is expressed using an unknown perturbation $\boldsymbol{\beta} = [\beta_1, \ldots, \beta_{N_r}]^T$ around the sampling grid as

$$\mathbf{z} = \boldsymbol{\Phi}(\check{\boldsymbol{\theta}}, \bar{\mathbf{r}} + \boldsymbol{\beta})\mathbf{p} + \sigma_w^2\mathbf{e},$$

with $-0.5\tau_r \leq \beta_n \leq 0.5\tau_r$ for $n = 1, \ldots, N_r$. We can now use the Taylor expansion as earlier to arrive at

$$\mathbf{z} = (\boldsymbol{\Phi}(\check{\boldsymbol{\theta}}, \bar{\mathbf{r}}) + \mathbf{D}\boldsymbol{\Delta}_\beta)\mathbf{p} + \sigma_w^2\mathbf{e}, \tag{20}$$

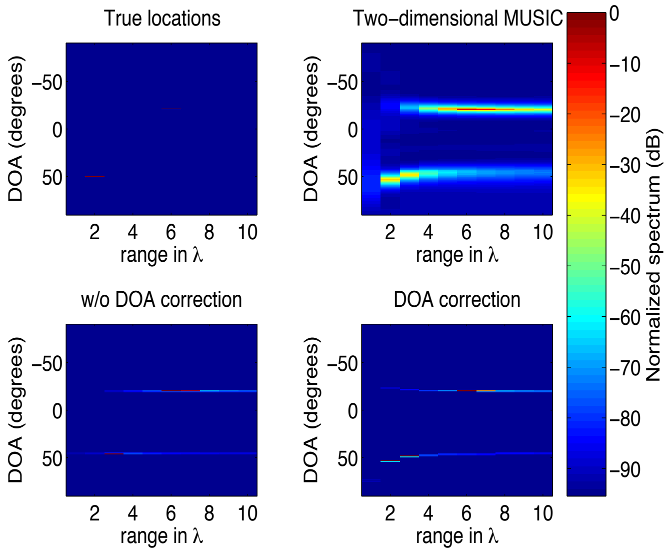

Fig. 2: Ignoring the grid mismatch: Sources located in the near-field at $(50.4°, 2.4\lambda)$ and Fresnel region at $(-20.6°, 6.2\lambda)$.

where $\mathbf{D} = [\frac{\partial \mathbf{\Phi}(\check{\theta}_1, \bar{r}_1)}{\partial \bar{r}_1}, \ldots, \frac{\partial \mathbf{\Phi}(\check{\theta}_{\hat{K}}, \bar{r}_1)}{\partial \bar{r}_1}, \ldots, \frac{\partial \mathbf{\Phi}(\check{\theta}_{\hat{K}}, \bar{r}_{N_r})}{\partial \bar{r}_{N_r}}] \in \mathbb{C}^{M^2 \times \hat{K} N_r}$, and $\mathbf{\Delta}_\beta = \mathrm{diag}(\boldsymbol{\beta} \otimes \mathbf{1}_{\hat{K}})$. Assuming that the spatial spectrum is sparse as earlier, the unknown $\mathbf{p}$ and $\boldsymbol{\beta}$ can be solved using the alternating minimization technique as in (14) or the joint sparse recovery technique as in (15).

V. Simulations

We consider a ULA with $M = 15$ sensors placed such that the inter-sensor spacing is $\delta = \lambda/4$, where λ represents the wavelength of the narrowband source signals. For such an array with $D = 3.5\lambda$, the near-field region is within 4.1λ, the Fresnel region is between 4.1λ and 24.5λ, and the far-field distance is beyond 24.5λ. We consider two sources, one in the near-field region at $(50.4°, 2.4\lambda)$ and the other in the Fresnel region at $(-20.6°, 6.2\lambda)$. The SNR is 0 dB with $T = 500$ snapshots. The sampling grid has a resolution of $\tau_\theta = 1°$ and $\tau_r = \lambda$. The chosen sampling grid does not include the two sources. The optimization problems in the proposed algorithms are solved using CVX [9]. The regularization parameters are chosen via cross-validation.

In Fig. 2, we ignore the mismatch effect, and estimate the DOA and range as if the targets are on the assumed grid. Source localization using the two-dimensional MUSIC [2] is based on the true model in (3) with $T = 500$ (without the Fresnel approximation). We solve (9) to estimate the DOA in step-1, and this is used directly without any correction to estimate the range. More specifically, we solve (19) with $\mathbf{\Phi}(\hat{\boldsymbol{\theta}}, \bar{\mathbf{r}})$. Alternatively, the estimated DOA obtained from step-1 is corrected by solving (17), and then the range is estimated by solving (19). This alleviates the Fresnel approximation error resulting in localization with a higher resolution compared to the MUSIC algorithm even at low SNRs. The energy leakage due to the grid mismatch can also be seen in Fig. 2.

In Fig. 3 and Fig. 4, we account for the off-grid sources. In Fig. 3, we use $\hat{\boldsymbol{\theta}}$ directly from step-1 to estimate the range in step-2 without any correction, i.e., the dictionary in (20) will

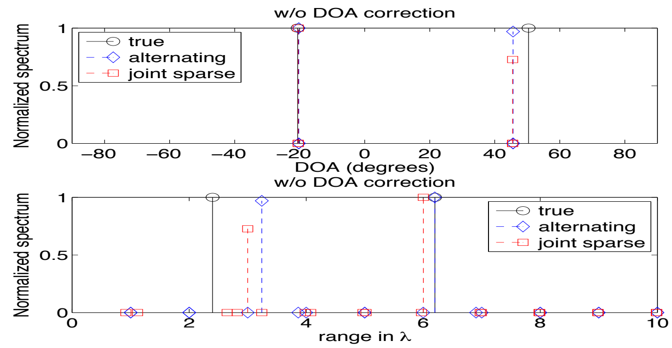

Fig. 3: Grid matching: sources located at $(50.4°, 2.4\lambda)$ and $(-20.6°, 6.2\lambda)$. The estimated DOA from step-1 is used for range estimation without any correction.

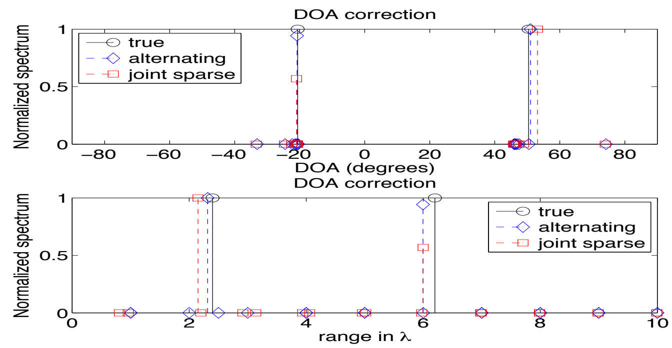

Fig. 4: Grid matching: sources located at $(50.4°, 2.4\lambda)$ and $(-20.6°, 6.2\lambda)$. The estimated DOA from step-1 is refined, and it is then used for range estimation.

be $\mathbf{\Phi}(\hat{\boldsymbol{\theta}}, \bar{\mathbf{r}})$. In Fig. 4, we correct the DOA by solving (17), which is then used for range estimation. The effect of the DOA correction is more significant when the sources are in the near-field rather than in the Fresnel region. The estimators based on alternating minimization have typically slow convergence as compared to the convex joint sparse estimators.

References

[1] H. Krim and M. Viberg, "Two decades of array signal processing research: the parametric approach," *IEEE Signal Process. Mag.*, vol. 13, no. 4, pp. 67–94, 1996.

[2] Y-D. Huang and M. Barkat, "Near-field multiple source localization by passive sensor array," *IEEE Trans. Antennas Propag.*, vol. 39, no. 7, pp. 968–974, Jul. 1991.

[3] A.L. Swindlehurst and T. Kailath, "Passive direction of arrival and range estimation for near-field sources," *IEEE Spec. Est. and Mod. Workshop*, pp. 123–128, 1988.

[4] Wanjun Zhi and M. Y W Chia, "Near-field source localization via symmetric subarrays," *IEEE Signal Process. Lett.*, vol. 14, no. 6, pp. 409–412, June 2007.

[5] K. Abed-Meraim, Y. Hua, and A. Belouchrani, "Second-order near-field source localization: algorithm and performance analysis," in *In proc. of the Asilomar Conference on Signals, Systems and Computers (ASILOMAR)*, Nov 1996, vol. 1, pp. 723–727 vol.1.

[6] Hao Zhu, G. Leus, and G.B. Giannakis, "Sparsity-cognizant total least-squares for perturbed compressive sampling," *IEEE Trans. Signal Process.*, vol. 59, no. 5, pp. 2002–2016, May 2011.

[7] R. Jagannath and K.V.S. Hari, "Block sparse estimator for grid matching in single snapshot DOA estimation," *IEEE Signal Process. Lett.*, vol. 20, no. 11, pp. 1038–1041, Nov 2013.

[8] Zhao Tan and A. Nehorai, "Sparse direction of arrival estimation using co-prime arrays with off-grid targets," *IEEE Signal Process. Lett.*, vol. 21, no. 1, pp. 26–29, Jan 2014.

[9] [Online], "CVX: Matlab software for disciplined convex programming, version 2.0 beta," http://cvxr.com/cvx, Sep. 2012.